Cao et al. BMC Cancer (2025) 25:443
https://doi.org/10.1186/s12885-025-13823-8

BMC Cancer

RESEARCH Open Access

Deep learning radiomics for the prediction of epidermal growth factor receptor mutation status based on MRI in brain metastasis from lung adenocarcinoma patients

Pingdong Cao[1], Xiao Jia[2], Xi Wang[3], Liyuan Fan[4], Zheng Chen[1], Yuanyuan Zhao[1], Jian Zhu[5] and Qiang Wen[1*]

Abstract

Background Early and accurate identification of epidermal growth factor receptor (EGFR) mutation status in non-small cell lung cancer (NSCLC) patients with brain metastases is critical for guiding targeted therapy. This study aimed to develop a deep learning radiomics model utilizing multi-sequence magnetic resonance imaging (MRI) to differentiate between EGFR mutant type (MT) and wild type (WT).

Methods In this retrospective study, 288 NSCLC patients with confirmed brain metastases were enrolled, including 106 with EGFR MT and 182 with EGFR WT. All patients were randomly divided into a training dataset (75%) and a validation dataset (25%). Radiomics and deep learning features were extracted from the brain metastatic lesions using contrast-enhanced T1-weighted (T1CE) and T2-weighted (T2W) MRI images. Features extraction and selection were performed using the least absolute shrinkage and selection operator (LASSO) and ResNet34. The predictive performance of the signatures for EGFR mutation status was assessed using receiver operating characteristic (ROC) curves and area under the curve (AUC) analyses.

Results No significant differences were found between the training and validation datasets. A four-feature radiomics signature (RS) demonstrated excellent predictive accuracy for EGFR MT, with α-binormal-based and empirical AUCs of 0.931 (95% CI: 0.880–0.940) and 0.926 (95% CI: 0.877–0.933), respectively. Incorporating deep learning signature (DLS) further enhanced the model's performance, achieving α-binormal-based and empirical AUCs of 0.943 (95% CI: 0.921–0.965) and 0.938 (95% CI: 0.914–0.962) in the training dataset. These findings were confirmed in the validation dataset, with AUCs of 0.936 (95% CI: 0.917–0.955) and 0.921 (95% CI: 0.901–0.941), demonstrating robust and consistent predictive performance.

Conclusions The multi-sequence MRI-based deep learning radiomics model exhibited high efficacy in predicting EGFR mutation status in NSCLC patients with brain metastases. This approach, which integrates advanced radiological features with deep learning techniques, offers a non-invasive and accurate method for determining EGFR mutation status, potentially guiding personalized treatment decisions in clinical practice.

*Correspondence:
Qiang Wen
wq890425@126.com

Full list of author information is available at the end of the article

© The Author(s) 2025. **Open Access** This article is licensed under a Creative Commons Attribution-NonCommercial-NoDerivatives 4.0 International License, which permits any non-commercial use, sharing, distribution and reproduction in any medium or format, as long as you give appropriate credit to the original author(s) and the source, provide a link to the Creative Commons licence, and indicate if you modified the licensed material. You do not have permission under this licence to share adapted material derived from this article or parts of it. The images or other third party material in this article are included in the article's Creative Commons licence, unless indicated otherwise in a credit line to the material. If material is not included in the article's Creative Commons licence and your intended use is not permitted by statutory regulation or exceeds the permitted use, you will need to obtain permission directly from the copyright holder. To view a copy of this licence, visit http://creativecommons.org/licenses/by-nc-nd/4.0/.

Keywords Radiomics, Deep learning, Magnetic resonance imaging, Epidermal growth factor receptor, Brain metastasis

Background

Lung cancer remains one of the leading causes of cancer-related mortality worldwide, with lung adenocarcinoma (LADC) accounting for approximately 50% of all cases [1]. Brain metastasis (BM) occurs in about 30% of lung cancer patients during the course of the disease, often leading to poor prognosis. The median overall survival for these patients is limited to only 7 months [2, 3]. Currently, several therapeutic approaches are available for managing lung cancer with BM, including chemotherapy, whole-brain radiotherapy (WBRT), stereotactic radiosurgery (SRS), and surgical resection. However, each of these approaches has its own limitations [4–6]. Chemotherapy is often ineffective against BM, primarily because chemotherapeutic agents have difficulty crossing the blood-brain barrier (BBB) and reaching the metastatic lesions [7]. WBRT and SRS are associated with potential side effects such as cerebral edema and cognitive decline [8]. Additionally, surgical resection can be effective in certain cases, but it is invasive and often fails to completely remove the metastatic lesions, leading to high recurrence rates [9, 10]. Given the limitations of current treatments, there is an urgent need to explore novel therapeutic strategies to better address BM in lung cancer patients.

Cancer treatment has entered the era of precision medicine, where genetic mutations and phenotypic variations play a crucial role in predicting clinical outcomes. In patients with locally advanced or advanced non-small cell lung cancer (NSCLC), targeted therapy has emerged as a more effective treatment option compared to conventional chemotherapy [11]. Among the various genetic alterations, epidermal growth factor receptor (EGFR) mutations are particularly significant, serving as independent risk factors for the development of BM. Notably, patients with EGFR MT are more prone to BM than those with the EGFR WT [12]. EGFR tyrosine kinase inhibitors (EGFR TKIs), small-molecule targeted agents, can partially cross the BBB and have shown substantial efficacy in treating brain metastases in EGFR-mutant NSCLC patients [13]. Therefore, accurately determining the EGFR mutation status of brain metastases is critical for tailoring treatment strategies, optimizing therapeutic outcomes, and ultimately improving patient prognosis.

Relying solely on the EGFR mutation status of the primary lung cancer to determine the mutation status of BM is often unreliable. Studies have shown that up to 30–53% of gene expression between primary tumors and brain metastases are inconsistent [14, 15]. Although biopsy and pathological examination remain the gold standard for confirming genotype, these methods have several limitations. Traditional biopsy techniques are invasive and may not be feasible for tumors located in certain anatomical regions. Furthermore, biopsies typically sample only a small portion of the tumor, which may not fully capture the heterogeneity of the entire lesion [16]. While circulating tumor DNA (ctDNA) analysis offers a non-invasive alternative, it is limited by the risks of false negatives and high costs [17, 18]. Therefore, to accurately assess the EGFR mutation status of brain metastases, biopsy or surgical resection followed by pathological examination is often necessary. However, these procedures carry inherent risks, including postoperative bleeding, pulmonary embolism, and cerebrospinal fluid leakage [19]. There is an urgent need to explore non-invasive methods for predicting the EGFR mutation status of brain metastases.

Magnetic resonance imaging (MRI) is an effective neuroimaging technique widely used for the detection, diagnosis, and monitoring of brain metastases. In the field of lung cancer, artificial intelligence (AI) has made significant strides, particularly in image analysis. Machine learning (ML) and deep learning (DL) techniques are capable of rapidly capturing tumor heterogeneity and extracting biological information that traditional visual inspection may not reveal [20]. These computational methods can uncover molecular and genetic insights that often exceed the capabilities of conventional imaging. Previous studies have primarily focused on CT imaging, using radiomics and deep learning to predict genetic mutations in lung cancer [21, 22]. Although studies by Mutic and Li et al. have shown that dual-modality MRI provides superior information and enhances predictive accuracy for genetic mutations compared to single-modality CT [23, 24], research on deep learning-based MRI analysis for predicting EGFR mutation status in brain metastases remains limited. In this retrospective study, we extracted conventional radiomics and deep learning features from T1 contrast-enhanced (T1-CE) and T2-weighted (T2W) MRI sequences. We then developed machine learning and deep learning models that integrate these features to differentiate between EGFR mutant (MT) and wild-type (WT) brain metastases.

Methods

Patient selection

Between January 2019 and December 2023, a total of 341 NSCLC patients with brain metastases were enrolled in this study. The inclusion criteria were as follows: (1) pathological diagnosis of NSCLC confirmed by biopsy or bronchoscopy; (2) baseline T2-weighted and

T1-weighted contrast-enhanced (T1-CE) MRI sequences obtained prior to anti-tumor treatment; (3) information on the specific EGFR mutation sites and mutation status; (4) tumors having a diameter greater than 5 mm. The exclusion criteria included: (1) incomplete clinical data, including but not limited to the lack of patient clinical factors and complete electronic medical records; (2) a history of malignancies other than NSCLC; (3) presence of central nervous system (CNS) disorders unrelated to cancer, including but not limited to cerebral infarction, traumatic brain injury, and neurodegenerative diseases such as Alzheimer's; (4) poor-quality or incomplete MRI scans due to artifacts or technical issues. After applying these inclusion and exclusion criteria, 288 patients were included in the final analysis. Clinical and genetic mutation information were obtained from the patients' electronic medical records. This study received approval from the Research Ethics Committee of Shandong Provincial Hospital affiliated with Shandong First Medical University. All procedures adhered to the guidelines and ethical principles outlined in the 1964 Helsinki Declaration. Informed consent was obtained from all participants.

Detection of EGFR mutation

Histopathological diagnoses of lung cancer were made for all patients based on samples collected via bronchoscopic or percutaneous needle-guided. Genomic DNA was extracted from formalin-fixed, paraffin-embedded (FFPE) tissue sections using the DNeasy Isolation Kit (Qiagen, Valencia, CA, USA). EGFR mutations were identified using the amplification refractory mutation system real-time PCR method with the Human EGFR Gene Mutation Detection Kit (Beijing ACCB Biotech Ltd).

Image acquisition and BM segmentation

Patients who were enrolled in this study were scanned at 3.0-T MRI scanner (Philips Medical Systems, Netherlands). Based on conventional sequences for diagnosing BM, we selected the following sequences and corresponding imaging acquisition parameters for analysis. The acquisition parameters of contrast-enhanced T1-weighted (T1CE) fast spin-echo sequence were as follows [25]: Repeat time = 250ms; Echo time = 2.46ms; matrix = 320 × 320; slice thickness = 5 mm; FOV = 240 × 240 mm. A T2-weighted sequence was obtained using a 3.0T MRI with TR = 4000 ms, TE = 113ms; slice thickness = 5 mm; FOV = 240 × 240 mm and matrix size = 352 × 352 mm. Additionally, the contrast agent utilized was gadolinium diethylenetriaminepentaacetic acid (Gd-DTPA, Bayer, Berlin, Germany). T1CE MR images were acquired 5 min post-injection of the contrast agent. The administered dosage was 0.2 mL/kg with an injection rate of 3 mL/s.

The two imaging sequences - T2-weighted and T1-CE were initially transformed into a uniform geometric space using the Elastix toolbox [26]. This registration step facilitated subsequent analyses and was executed via the open-source 3D Slicer software platform (Version 4.10, http://www.slicer.org). Regions of interest (ROIs) were automatically contoured using AccuContour software (version 3.0, Manteia Medical Technologies Co. Ltd., Xiamen, China) based on deep learning algorithms, then manually modified by the first radiologist with 7 years' experience and the second radiologist with 10 years of experience. Lesions with a diameter less than 5 mm were not included. Two independent radiologists were blinded to the clinicopathological information. Any disagreement of 5% or more was resolved through consensus [27, 28].

Radiomics features and deep learning features extraction

Quantitative radiomics feature extraction was automatically performed with PyRadiomics packages, which enable feature calculation in 3D Slicer software (Version 4.10, http://www.slicer.org). 93 features were extracted from each ROI and included first-order intensity histogram (IH) and statistical matrix (SM) features, grey-level co-occurrence matrix (GLCM), gray-level run-length matrix (GLRLM), gray-level size zone matrix (GLSZM), neighboring gray-tone difference matrix (NGTDM), and gray-level dependence matrix (GLDM) features. Furthermore, 744 wavelet features were extracted for IH and SM from 8 wavelet decompositions. All radiomic features were z-score normalized to a mean of 0 and a standard deviation of 1. To evaluate intra-observer reproducibility, two radiologists independently segmented 25 randomly selected lesions from the dataset. The radiomic features extracted from the two independently drawn ROIs were compared using intra-class correlation coefficients (ICCs). Features exhibiting an ICC ≥ 0.8 were retained, and features with an ICC < 0.8 were initially excluded from further analyses due to unsatisfactory intra-observer reproducibility.

The processed tumor images served as input for convolutional neural network (CNN) models. For this investigation, we employed ResNet34 as our pre-trained CNN architecture. This model is a variant of the Residual Network (ResNet) family, designed to mitigate the challenges of gradient vanishing and exploding during deep network training. ResNet34 achieves this through the incorporation of skip connections, allowing the network to learn residual functions with reference to the layer inputs, thereby facilitating the training of deeper neural networks [29]. The network takes a 224 × 224 × 3-pixel natural image as input and, after multiple consecutive convolutional and pooling layers, outputs a 1,000-dimensional vector, which we considered the deep feature extracted from the image. The weights were pretrained

using the open-source dataset ImageNet-1k (https://www.image-net.org/download.php). These slices, including the central tumor slice and two adjacent slices on either side, and the ROI regions were extracted. To ensure data quality, all samples underwent manual inspection to verify image integrity and exclude partial volume artifacts. These images were resized to 224 × 224 using bilinear interpolation and replicated across 3 channels for input into ResNet34. After inputting the ROI images into the model, a 1,000-dimensional deep feature was extracted from each ROI region of each sequence.

Features selection

Feature selection technique was implemented to pinpoint and exclude irrelevant radiomic features that could potentially impair the predictive performance for differentiating EGFR MT and WT in the following three steps. First, the Mann–Whitney U test was performed to each feature, and features with $p < 0.05$ were retained. Then, to mitigate the risks of overfitting and selection bias, the least absolute shrinkage and selection operator (LASSO) [30], a machine learning technique, was employed for optimal feature selection. The objective was to identify the most discriminative radiomic features capable of distinguishing EGFR MT and WT. For the binary logistic regression model, the tuning parameter λ in LASSO was determined through 5-fold cross-validation, minimizing the criteria using the "glmnet" package in R software (Version 3.4, http://www.r-project.org/) [31]. All wavelet filtering, image preprocessing, and subsequent radiomics analysis were conducted using the Multimodal Radiomics Platform, as described in prior publications (accessible online [32]: http://cfu.lab.nycu.edu.tw/MRP_MLinglioma.html). The Akaike Information Criterion (AIC) was used as the evaluation index, and the optimal feature subset was obtained using the backward stepwise search algorithm.

Model construction and validation for EGFR mutation status

After feature selection, we developed a logistic regression model to validate the effectiveness of the selected radiomics features and deep learning features. The signature was computed as a linear combination of the selected features, weighted by their respective LASSO coefficients in the training group. The stacking fusion method was used to construct the DLR signature in a logistic regression model to predict the mutation status of EGFR. Sample size limitations and uneven group distributions can introduce bias, potentially distorting performance estimates. In cases of imbalanced datasets, traditional ROC curve analysis may yield misleadingly high AUC values, obscuring true model efficacy. To address this issue, we employed precision-recall curves (PRC), which plot positive predictive value against true positive rate across all thresholds. The area under the PRC, termed average precision (AP), provides a more robust evaluation metric for imbalanced classification tasks, offering complementary insights to conventional receiver operating characteristics (ROC) analysis. We employed an α-binormal model to generate smooth ROC and precision-recall curves, addressing previous limitations. The model's discriminative ability was evaluated using these curves. Developed on the training dataset and validated independently, the model yielded total points for each patient, facilitating comprehensive assessment across cohorts. Generally, to evaluate the predictive performance of the signatures, ROC analysis, decision curve analysis and calibration curve analysis were conducted to evaluate the model's accuracy and clinical applicability.

Statistics analysis

Statistical analysis was performed using R software version 3.4.2 (Auckland, New Zealand). Statistical analyses were conducted using appropriate tests for categorical and continuous variables. Chi-squared or Fisher's exact tests were applied for clinical categorical factors, such as gender, ECOG PS status and smoking history etc. While Mann-Whitney U tests were used for continuous variables, involving ages and preliminary selecting for distinguishing features of EGFR mutation statuses. The "rms" and "pROC" R packages were utilized to generate comparison, calibration, and precision-recall curves, providing comprehensive visual representations of model performance. The "glmnet" package was used to execute the LASSO algorithm, and the "pROC" package was used to assess predictive values. All statistical analyses were two-sided, and a p-value < 0.05 was considered statistically significant.

Results

Patient characteristics

A total of 288 EGFR positive NSCLC patients with brain metastasis were included in this retrospective study. The training set consisted of 83 patients with EGFR MT and 133 patients with EGFR WT. The validation set included 23 patients with EGFR MT and 49 patients with EGFR WT mutations. The median age at baseline was 61.4 ± 12.3 and 62.8 ± 11.7 in training and validation datasets, respectively ($p = 0.761$). Demographic and clinical characteristics, including smoking history ($p = 0.415$), ECOG PS ($p = 0.674$), gender ($p = 0.463$), and genetic mutation profile ($p = 0.323$), were comparable across both cohorts, with no statistically significant differences observed. Table 1 summarizes the clinical characteristics of the patients, while Table 2 presents the clinicopathological factors of patients in the training set, specifically with regard to EGFR mutation status. No significant

Table 1 Clinical factors of patients in the training and validation datasets

Characteristic	Training dataset	Validation dataset	*p*-value
Gender			0.463
Male	151	47	
Female	65	25	
Age	61.4 ± 12.3	62.8 ± 11.7	0.761
ECOG PS			0.674
0–1	132	46	
2	84	26	
Smoking History			0.415
Yes	177	62	
No	39	10	
EGFR Subtype			0.323
MT	83	23	
WT	133	49	

Abbreviation: ECOG PS: Eastern cooperative oncology group performance status, EGFR: Epidermal growth factor receptor

Table 2 Clinical factors of patients with EGFR MT and EGFR WT status in the training dataset

Characteristic	EGFR MT	EGFR WT	*p*-value
Gender			0.364
Male	61	90	
Female	22	43	
Age	60.2 ± 10.8	62.6 ± 13.5	0.441
ECOG PS			0.513
0–1	53	79	
2	30	54	
Smoking History			0.470
Yes	70	107	
No	13	26	

Abbreviation: ECOG PS: Eastern cooperative oncology group performance status, EGFR: Epidermal growth factor receptor

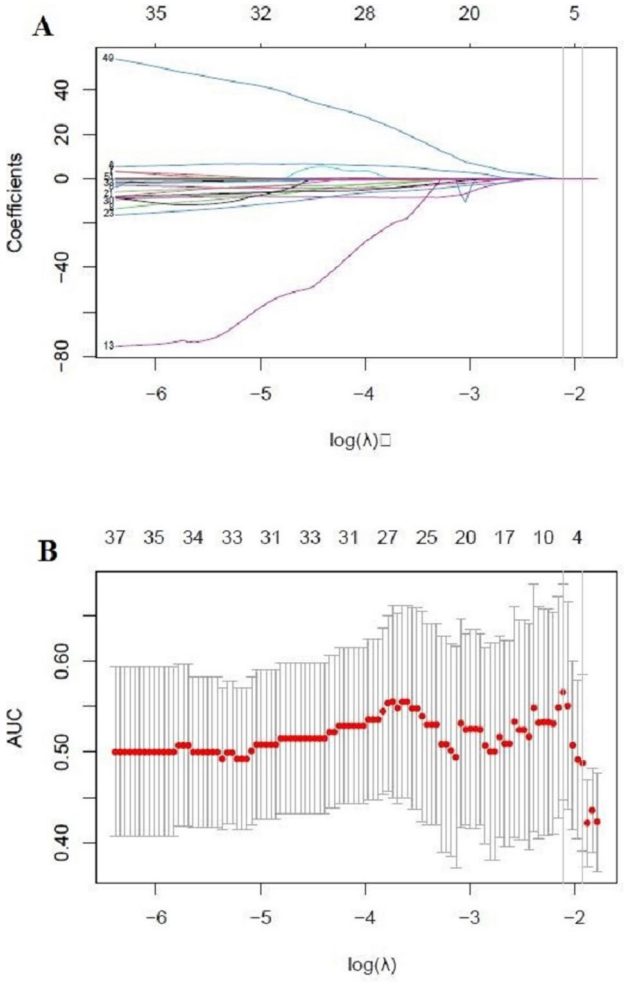

Fig. 1 Radiomics features selection through LASSO with a binary regression model. (A) The LASSO coefficient profile plot was produced against the log lambda sequence. (B) Tuning parameter (log lambda) selection in the LASSO via minimum criteria. AUC: Area under the curve

predictive value for EGFR mutation status was found for gender ($p = 0.364$) or ECOG PS ($p = 0.513$). Additionally, smoking history did not reveal any statistically significant differences when identifying EGFR mutant status ($p = 0.470$).

Radiomics signatures construction and validation

The radiomics analysis included 837 features extracted from segmented pretreatment MRI images of patients. After applying an interclass correlation coefficient cut-off value of 0.8 for the reproducibility test, 541 features were retained for further analysis. LASSO regression identified four radiomics features with non-zero coefficients, which were used to construct the signature in the training set. As illustrated in Fig. 1, these features were weighted according to their respective coefficients. The radiomics signature (RS) demonstrated high discriminative power between EGFR MT and EGFR WT. In the training set, the signature achieved α-binormal and empirical AUCs of 0.931 (95% CI: 0.880–0.940) and 0.926 (95% CI: 0.877–0.933), respectively. This robust performance was further validated in the independent cohort, yielding even higher AUCs (α-binormal: 0.892 (95% CI: 0.870–0.913), empirical: 0.887 (95% CI: 0.865–0.908)). Table 3 summarizes these results, including the average precision (AP) values. Overall, the model developed based on brain metastasis MR images demonstrated robust capability in discriminating EGFR mutation phenotypes in lung cancer (Fig. 2).

Deep learning signature construction and validation

LASSO regression analysis reduced the deep learning-derived features from 1520 to 16 potential predictors, retaining only those with non-zero coefficients. We developed a model by deep learning features obtained from the optimized imaging model. The deep learning signature (DLS) model demonstrated superior predictive efficacy for differentiating EGFR mutation phenotypes

Table 3 The predictive performances of RS for EGFR mutant status

Performance	Training dataset				Validation dataset			
	$AUC_{\alpha-bin}$	AUC_{emp}	$AP_{\alpha-bin}$	AP_{emp}	$AUC_{\alpha-bin}$	AUC_{emp}	$AP_{\alpha-bin}$	AP_{emp}
RS	0.931	0.926	0.896	0.882	0.892	0.887	0.854	0.823
95% CI	0.880–0.940	0.877–0.933	0.877–0.914	0.866–0.898	0.870–0.913	0.865–0.908	0.834–0.873	0.790–0.853
p-value	< 0.001	< 0.001	< 0.001	< 0.001	< 0.001	< 0.001	< 0.001	< 0.001

Abbreviation: RS: Radiomics signature, AUC: Area under the curve, AP: Average precision, $AUC_{\alpha-bin}$: The α-binormal area under the curve, AUC_{emp}: The empirical area under the curve, $AP_{\alpha-bin}$: The α-binormal average precision, AP_{emp}: The empirical average precision

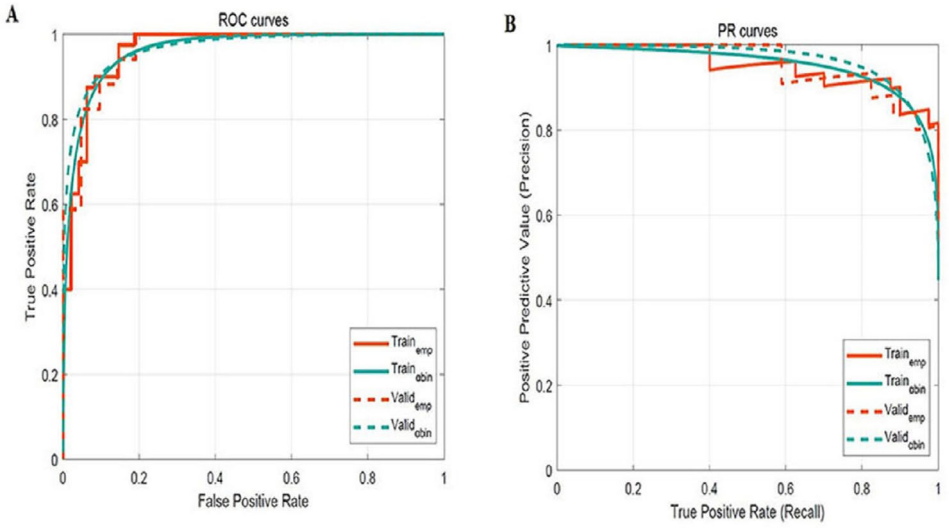

Fig. 2 The performances of the developed radiomics signature. (A) Receiver operating characteristics (ROC) curves. (B) Precision-recall curve (PRC)

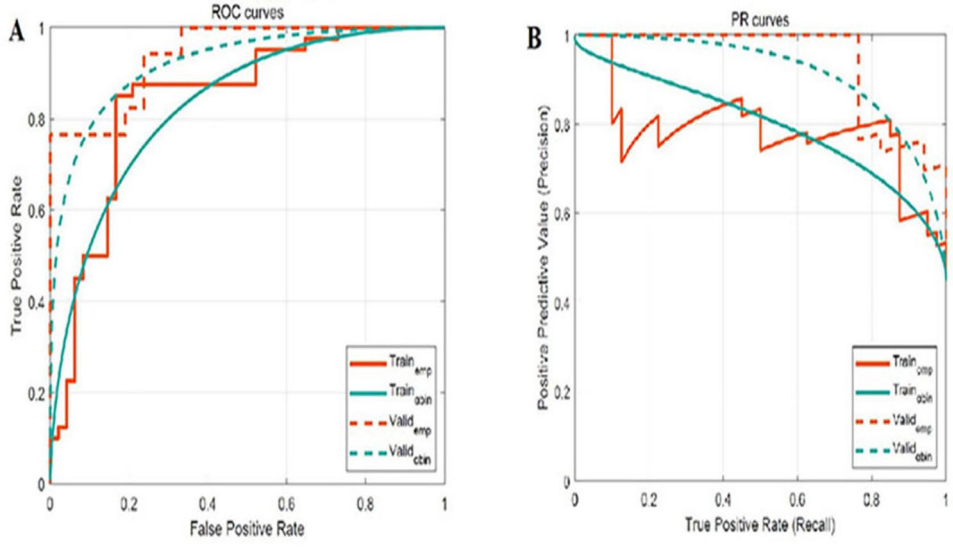

Fig. 3 The performance of the developed deep learning signatures. (A) Receiver operating characteristics (ROC) curves. (B) Precision-recall curve (PRC). The performance of the developed deep learning signatures. (A) Receiver operating characteristics (ROC) curves. (B) Precision-recall curve (PRC)

compared to the RS alone. In the training cohort, it achieved the highest AUC with α-binormal and empirical AUCs of 0.943 (95% CI: 0.921–0.965) and 0.938 (95% CI: 0.914–0.962), respectively, highlighting its robust discriminative capability. External validation of the model in an independent cohort confirmed its exceptional discriminative performance, yielding an α-binormal AUC of 0.936 and an empirical AUC of 0.921 (95% CI: 0.901–0.941) (Fig. 3) (Table 4).

The calibration curve indicated a strong concordance between the predicted EGFR mutation status probability and the actual observed outcomes using restricted

Table 4 The predictive performances of DLS for EGFR mutant status

Performance	Training dataset				Validation dataset			
	$AUC_{\alpha-bin}$	AUC_{emp}	$AP_{\alpha-bin}$	AP_{emp}	$AUC_{\alpha-bin}$	AUC_{emp}	$AP_{\alpha-bin}$	AP_{emp}
DLS	0.943	0.938	0.936	0.917	0.936	0.921	0.905	0.895
95% CI	0.921–0.965	0.914–0.962	0.918–0.954	0.897–0.937	0.917–0.955	0.901–0.941	0.885–0.925	0.871–0.919
p-value	< 0.001	< 0.001	< 0.001	< 0.001	< 0.001	< 0.001	< 0.001	< 0.001

Abbreviation: DLS: Deep learning signature, AUC: Area under the curve, AP: Average precision, $AUC_{\alpha-bin}$: The α-binormal area under the curve, AUC_{emp}: The empirical area under the curve, $AP_{\alpha-bin}$: The α-binormal average precision, AP_{emp}: The empirical average precision

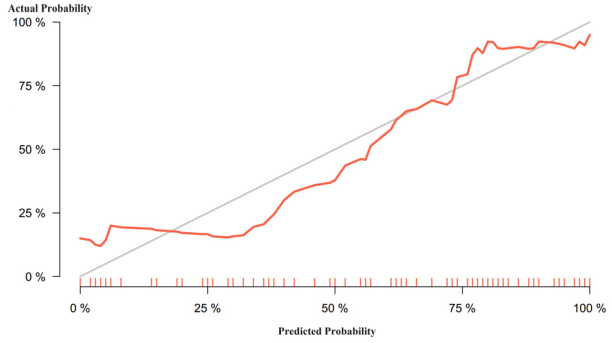

Fig. 4 Calibration curve of the deep learning signatures shows as a red line

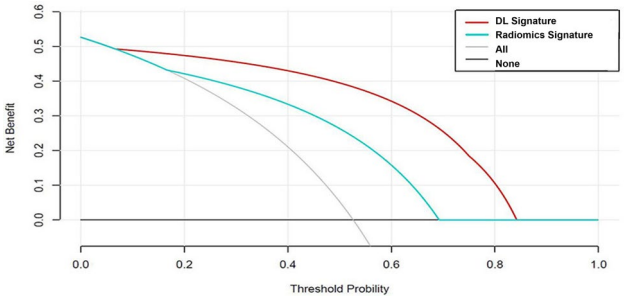

Fig. 5 The decision of the radiomics signature, deep learning signatures and two extreme curves were plotted based on the validation dataset. The figure illustrated that the utilize of deep learning signatures to predict EGFR MT has a greater benefit that the radiomics signature alone

cubic splines, with an AUC of 0.870 (95% CI: 0.781–0.959) (Fig. 4). The degree of alignment of the calibration curve with the diagonal line was directly related to the DLS's predictive accuracy. This close alignment signifies that the DLS's predictions were highly reliable. To further evaluate clinical utility, decision curves for both the RS and the DLS were plotted. These decision curves illustrated the net benefit of each signature across a range of threshold probabilities. Figure 5 confirmed that DLS exhibited superior performance in distinguishing between EGFR WT and MT cases, providing a greater net benefit compared to the RS.

Discussion

In the era of precision medicine, the rapid and accurate prediction of EGFR mutations is crucial for implementing targeted therapies, as it enables clinicians to tailor treatment plans based on the patient's specific mutation profile, thereby significantly improving therapeutic outcomes. In this study, we used LASSO and ResNet34 to extract and select features, demonstrating the potential of MRI images in predicting the EGFR mutation status in lung adenocarcinoma patients with brain metastases. More importantly, we developed a deep learning-based predictive model designed to assist clinicians in forecasting EGFR mutation status, providing an effective tool to enhance treatment precision in this complex clinical context.

Brain metastasis is a common and serious complication in lung cancer, accounting for 40–50% of all brain metastasis cases [33]. EGFR mutations are associated with a higher risk of brain metastasis in NSCLC patients [34, 35], and EGFR TKIs have shown significant efficacy in treating brain metastases, making them a viable first-line treatment option [36]. EGFR-mutated patients should be prioritized for targeted therapy, while wild-type patients need to assess PD-L1 expression and select appropriate local treatments [37]. The effectiveness of treating central nervous system metastases largely depends on the ability of drugs to penetrate BM. Drug distribution is influenced by factors such as BBB disruption, tumor growth characteristics, and the activity of efflux transporters [38, 39]. EGFR TKIs have demonstrated significant efficacy in treating brain metastases in EGFR-mutated patients, with first- and second-generation EGFR inhibitors changing the treatment landscape for NSCLC [40]. Third-generation TKIs, such as osimertinib, effectively overcome resistance caused by the EGFR T790M mutation and can penetrate both the blood-brain barrier and blood-tumor barrier [41, 42]. These findings underscore the importance of studying EGFR mutation subtypes to guide personalized treatment strategies.

In clinical practice, the evaluation of EGFR mutation status typically relies on two methods: plasma ctDNA detection and tissue biopsy, each of which has its inherent limitations. Plasma ctDNA detection, while non-invasive and convenient, is often limited by the low concentration of ctDNA in plasma, and the high costs associated with the procedure are significant barriers to its widespread use [18, 43, 44]. In contrast, tissue biopsy provides direct genomic information but is an invasive procedure that carries risks, such as vascular or neural

damage, and the potential for tumor cell dissemination. Furthermore, biopsy samples are typically obtained from a specific region of the lesion, which may not fully capture the heterogeneity of the entire tumor [45]. In situations where pathological sampling is not feasible, MRI analysis of brain metastases offers an effective alternative for predicting the type of EGFR mutation, thereby improving diagnostic accuracy and providing valuable insights for the development of personalized treatment strategies [46].

Radiomics-based binary classification models have shown significant potential in predicting EGFR mutation status by automating the extraction of features from medical imaging data. Liu et al. demonstrated that integrating CT radiomics features with clinical data enhanced the predictive power for EGFR mutation in a cohort of 298 lung adenocarcinoma patients, improving the AUC from 0.690 to 0.778 [47]. Similarly, Zhao et al. achieved an increase in AUC from 0.645 to 0.758 by combining CT radiomics features with deep learning techniques [48]. However, CT-based deep learning models face several inherent limitations. A major obstacle is the accurate delineation and segmentation of lung lesions in CT images, particularly when complex anatomical structures such as major blood vessels, lymph nodes, and adjacent organs are involved. These complexities can impair the accuracy of segmentation and adversely affect model performance [49–51]. In contrast, MRI offers distinct advantages over CT in this application, including superior soft tissue contrast and the ability to capture multiple sequence parameters [23, 52]. These advantages of MRI may enhance the accuracy and robustness of radiomics-based prediction models for EGFR mutation status, providing a more reliable alternative for clinical use.

Our research focuses on the radiomic analysis of MRI images of brain metastases, differentiating from previous studies that primarily concentrated on CT radiomics of primary lung tumors. Previous studies have explored the application of deep learning models based on MRI for predicting EGFR mutation status. Wang et al. evaluated a radiomic signature for predicting two EGFR subtypes but reported unsatisfactory results, with low AUCs [46]. Li et al. demonstrated that a deep learning approach using multi-sequence MRI could predict EGFR mutation status in NSCLC patients with brain metastases [53]. However, their study lacked external validation and only provided a basic distinction between EGFR mutations and wild-type status. Our encouraging results can be attributed to the following two factors. First, we selected lesions with a diameter greater than 5 mm to avoid the potential influence of noise, blurring, or low contrast, which could hinder the accurate identification of boundaries by segmentation algorithms. This is particularly important in low-resolution or unclear medical images, where small tumors may be misclassified as background or other structures. Furthermore, the chosen segmentation approach combines automatic segmentation with manual adjustments by experienced physicians. Traditional threshold-based segmentation algorithms may perform well for large tumors but often fail to detect smaller ones. In contrast, deep learning-based algorithms, by learning more complex features, can adapt to segmentation tasks involving tumors of varying sizes. This approach not only reduces errors inherent in purely manual segmentation but also enhances labelling consistency and repeatability. Third, the application of advanced ROIs segmentation algorithms. Enhancing the accuracy of these segmentation algorithms is currently crucial for improving the performance of medical image analysis and predictive models. Research on tumor segmentation has been conducted across various tumor types, with a particular emphasis on methods designed to enhance segmentation accuracy in complex anatomical areas and small regions. Mudassar et al. combined an attention-enhanced U-Net model with cGAN, achieving two key breakthroughs: the block discriminator in cGAN can generate highly realistic synthetic images for data augmentation, addressing the limitation of annotated data availability; and the attention mechanism embedded in U-Net can accurately capture complex structural features, such as tumor boundaries [54]. This approach performed excellently on the brain MRI dataset, achieving a Dice coefficient of 98.61%. Nomura et al. developed an adaptive input strategy based on fixed-size VOI (Volume of Interest), enabling the model to handle lesions of varying sizes [55]. When applied to brain metastasis tumor segmentation, the Dice coefficient was 0.727 ± 0.115. Therefore, future research may focus on developing adaptive algorithms that automatically adjust to tumor size variations, combined with multi-scale and multi-task learning approaches, to further improve segmentation accuracy and prediction performance.

With the widespread adoption of technologies such as CNNs and Deep Neural Networks (DNNs), numerous studies have shown that deep learning surpasses traditional radiomics signatures in distinguishing EGFR mutations. Song et al. reported that deep learning-based methods outperformed radiomics in classifying EGFR mutation subtypes in lung adenocarcinoma patients [56]. Similarly, research by Nguyen et al. confirmed these findings, demonstrating that deep learning algorithms performed better than conventional machine learning (cML), achieving higher AUC (0.822 vs. 0.775) and sensitivity (80.1% vs. 71.1%) [57]. Our findings are consistent with these studies. By integrating deep neural networks, MRI quantitative features, and EGFR genetic data, our DeepSurv model accurately predicts the EGFR mutation status of patients based on imaging features,

demonstrating its potential in survival analysis. Additionally, we have addressed the challenge of small labeled medical image datasets through multi-sequence image fusion. Moreover, deep learning models that incorporate genomic mutation data show greater prognostic accuracy compared to traditional clinical staging, highlighting the crucial role of sequence mutation analysis in advancing molecular typing for lung cancer.

Several factors can influence the accuracy of predictive models. Ahn et al.'s study suggests that diagnosing EGFR mutation status in large brain metastases (diameter > 10 mm) may be less effective than in smaller lesions, possibly due to the presence of necrotic centers, which can impair the accuracy of machine learning classifications [58]. Additionally, large brain metastases often correspond to smaller datasets, which may lead to overfitting issues. In contrast, Zhou et al. pointed out that accurately genotyping EGFR mutations in patients with small brain metastases is challenging, primarily due to the difficulty in extracting imaging features from these very small lesions [59]. Previous studies have also emphasized the importance of the metastasis/brain parenchyma (M/BP) interface in predicting EGFR mutations. Fan et al. demonstrated that the M/BP interface and the tumor's active regions could provide complementary information regarding EGFR mutation status and response to EGFR-TKI therapy [60]. The complexity of peritumoral edema, especially in irregularly shaped lesions, may also affect image segmentation accuracy, making precise delineation more difficult. Moreover, brain metastases exhibit diverse imaging characteristics across different brain regions (e.g., cerebrum, cerebellum, meninges), which complicates the development of unified predictive models and highlights the need for region-specific analytical approaches. Future research should focus on addressing these challenges to enhance the accuracy of prediction models and their applicability in clinical decision-making.

In this study, the model demonstrated exceptional predictive accuracy for EGFR mutations, with α-binormal-based and empirical AUCs of 0.931 and 0.926, respectively. These results were also confirmed in the validation dataset. Notably, our approach utilized multi-center data while maintaining high predictive accuracy, which underscores the model's strong generalization capabilities. Both our study results and the prediction models constructed using deeper features show that their predictive performance is influenced not only by the segmentation algorithm but also by other factors. The imaging protocol during MRI acquisition can affect the extraction and values of radiomics or deep learning features, such as voltage, current, and image slice thickness. We applied the LASSO algorithm to eliminate features with high correlation, redundancy, or instability, thereby selecting the optimal features to enhance the predictive performance of deep learning and machine learning models. The value of the feature parameters identified in this study in other research remains to be validated, but these factors have the potential to improve predictive performance. Conversely, the conclusions and parameters from previous studies have only been validated within specific datasets, and their applicability in our study requires further validation.

This study has several limitations that warrant further consideration. Firstly, the retrospective design of the study inherently introduces the potential for selection bias. Secondly, tumor segmentation on the MRI images was performed using a semi-automatic approach by a multidisciplinary team of experienced radiologists and oncologists. Future development of fully automated segmentation methods could not only reduce the time and cost associated with treatment planning but also improve the reproducibility of radiomic features. Thirdly, due to the relatively small sample size, this study did not predict different EGFR mutation subtypes. Future research could focus on predicting the prognosis of different EGFR mutation sites, such as 19 del, L858R, T790M, and related TKI treatments.

Conclusions

In conclusion, our study highlights the effectiveness of a multisequence MRI-based model in predicting EGFR mutation status in metastatic NSCLC patients. By integrating complex radiological features with advanced machine learning techniques, this novel approach provides a non-invasive and accurate method for determining EGFR mutation status. The model shows significant potential as a valuable clinical decision support tool, especially in cases where biopsy is difficult or contraindicated.

Abbreviations

CT	Computed tomography
LADC	Lung adenocarcinoma
LC	Lung cancer
NSCLC	Non-small cell lung cancer
BM	Brain metastasis
BBB	Blood-brain barrier
EGFR	Epidermal growth factor receptor
BMs	Brain metastases
TKIs	Tyrosine kinase inhibitors
ctDNA	Circulating tumor DNA
CT	Computed tomography
MRI	Magnetic resonance imaging
CR	Conventional radiomics
DL	Deep learning
CNS	Central nervous system
T1CE	Contrast-enhanced T1-weighted
T2W	T2-weighted
IH	Intensity histogram
SM	Statistical matrix
GLCM	Grey-level co-occurrence matrix
GLRLM	Gray-level run-length matrix
GLSZM	Gray-level size zone matrix

NGTDM	Neighboring gray-tone difference matrix
GLDM	Gray-level dependence matrix
ICCs	Interclass correlation coefficients
CNN	Convolutional neural network
ResNet	Residual Network
ROIs	Regions of interesting
LASSO	Least absolute shrinkage and selection operator
AIC	Akaike Information Criterion
DLR	Deep Learning Radiomics
PRC	Precision-recall curves
AP	Average precision
ROC	Receiver operating characteristics
RS	Radiomics signature
AUC	Area under the curve
pCR	Pathological complete response
DRS	Distant Recurrence Score
WT	Wild-type
DNNs	Deep Neural Networks
cML	Conventional machine learning
M/BP	Metastasis/brain parenchyma

Acknowledgements
Not Applicable.

Author contributions
Q. W and PD. C designed the study and wrote the manuscript. Z. C participated in the study designing and data collection. X. W and X. J provided the analysis of data and ROI segmentation. YY.Z and LY.F participated in data collection and offered guidance. J. Z provided assistance in revising the manuscript. Q. W carried out the study design and interpretation of data and drafted the manuscript. All authors contributed to the article and approved the submitted version.

Funding
This study was supported by Shandong Province Medical Staff Science and Technology Innovation Program (grant number SDYWZGKCJH2022018), Shandong Medical Association Clinical Research Fund–Qilu Special Project (grant number YXH2022ZX02196), Jinan Science and Technology Clinical Medicine Innovation Plan (grant number 20225011 and 20238073) and Shandong Provincial Natural Science Foundation (grant numbers ZR2024MH268). The funding sources had no role in the study design, data collection, analysis of interpretation, or writing of this manuscript.

Data availability
The datasets generated or analyzed during the study are available from the corresponding author on reasonable request.

Declarations

Ethics approval and consent to participate
This study received approval from the Research Ethics Committee of Shandong Provincial Hospital Affiliated to Shandong First Medical University. Ethical approve of present study was obtained from the Institutional Review Board. Meanwhile, this study was conducted in accordance with the Declaration of Helsinki (as revised in 2013). Informed consent was obtained from all participants.

Consent for publication
Not Applicable.

Competing interests
The authors declare no competing interests.

Author details
[1]Department of Radiation Oncology, Shandong Provincial Hospital Affiliated to Shandong First Medical University, Shandong First Medical University, Jinan, China
[2]School of Control Science and Engineering, Shandong University, Jinan, China
[3]Department of Radiation Oncology, Stanford University, Palo Alto 94305, USA
[4]Department of Radiation Oncology, Qilu Hospital of Shandong University, Jinan 250021, China
[5]Department of Radiation Physics and Technology, Shandong Cancer Hospital and Institute, Jinan 250021, China

Received: 22 July 2024 / Accepted: 26 February 2025
Published online: 12 March 2025

References

1. Brainard J, Farver C. The diagnosis of non-small cell lung cancer in the molecular era. Mod Pathol. 2019;32:16–26.
2. Berghoff AS, Schur S, Füreder LM, Gatterbauer B, Dieckmann K, Widhalm G, Hainfellner J, Zielinski CC, Birner P, Bartsch R. Descriptive statistical analysis of a real life cohort of 2419 patients with brain metastases of solid cancers. ESMO Open. 2016;1(2):e000024.
3. Hartgerink D, Van der Heijden B, De Ruysscher D, Postma A, Ackermans L, Hoeben A, Anten M, Lambin P, Terhaag K, Jochems A. Stereotactic radiosurgery in the management of patients with brain metastases of non-small cell lung cancer: indications, decision tools and future directions. Front Oncol. 2018;8:154.
4. Winther RR, Hjermstad MJ, Skovlund E, Aass N, Helseth E, Kaasa S, Yri OE, Vik-Mo EO. Surgery for brain metastases—impact of the extent of resection. Acta Neurochir. 2022;164(10):2773–80.
5. Minniti G, Niyazi M, Andratschke N, Guckenberger M, Palmer JD, Shih HA, Lo SS, Soltys S, Russo I, Brown PD. Current status and recent advances in resection cavity irradiation of brain metastases. Radiat Oncol. 2021;16:1–14.
6. Suh JH, Kotecha R, Chao ST, Ahluwalia MS, Sahgal A, Chang EL. Current approaches to the management of brain metastases. Nat Reviews Clin Oncol. 2020;17(5):279–99.
7. Papademetriou IT, Porter T. Promising approaches to circumvent the blood–brain barrier: progress, pitfalls and clinical prospects in brain cancer. Therapeutic Delivery. 2015;6(8):989–1016.
8. Brown PD, Jaeckle K, Ballman KV, Farace E, Cerhan JH, Anderson SK, Carrero XW, Barker FG, Deming R, Burri SH. Effect of radiosurgery alone vs radiosurgery with whole brain radiation therapy on cognitive function in patients with 1 to 3 brain metastases: a randomized clinical trial. JAMA. 2016;316(4):401–9.
9. Sahgal A, Aoyama H, Kocher M, Neupane B, Collette S, Tago M, Shaw P, Beyene J, Chang EL. Phase 3 trials of stereotactic radiosurgery with or without whole-brain radiation therapy for 1 to 4 brain metastases: individual patient data meta-analysis. Int J Radiation Oncology* Biology* Phys. 2015;91(4):710–7.
10. Minniti G, Clarke E, Lanzetta G, Osti MF, Trasimeni G, Bozzao A, Romano A, Enrici RM. Stereotactic radiosurgery for brain metastases: analysis of outcome and risk of brain radionecrosis. Radiat Oncol. 2011;6:1–9.
11. Arbour KC, Riely GJ. Systemic therapy for locally advanced and metastatic non–small cell lung cancer: a review. JAMA. 2019;322(8):764–74.
12. Rangachari D, Yamaguchi N, VanderLaan PA, Folch E, Mahadevan A, Floyd SR, Uhlmann EJ, Wong ET, Dahlberg SE, Huberman MS. Brain metastases in patients with EGFR-mutated or ALK-rearranged non-small-cell lung cancers. Lung Cancer. 2015;88(1):108–11.
13. Rybarczyk-Kasiuchnicz A, Ramlau R, Stencel K. Treatment of brain metastases of non-small cell lung carcinoma. Int J Mol Sci. 2021;22(2):593.
14. Bozzetti C, Tiseo M, Lagrasta C, Nizzoli R, Guazzi A, Leonardi F, Gasparro D, Spiritelli E, Rusca M, Carbognani P. Comparison between epidermal growth factor receptor (EGFR) gene expression in primary non-small cell lung cancer (NSCLC) and in fine-needle aspirates from distant metastatic sites. J Thorac Oncol. 2008;3(1):18–22.
15. Brastianos PK, Carter SL, Santagata S, Cahill DP, Taylor-Weiner A, Jones RT, Van Allen EM, Lawrence MS, Horowitz PM, Cibulskis K. Genomic characterization of brain metastases reveals branched evolution and potential therapeutic targets. Cancer Discov. 2015;5(11):1164–77.
16. Wen Q, Yang Z, Zhu J, Qiu Q, Dai H, Feng A, Xing L. Pretreatment CT-based radiomics signature as a potential imaging biomarker for predicting the expression of PD-L1 and CD8 + TILs in ESCC. OncoTargets Therapy 2020 ; 12003–13.
17. Fan L, Li M, Zhou X, Jia X, Tian H, Wen Q. T cell-related circrna pairs to predict prognosis of patients with esophageal squamous cell carcinoma. Int Immunopharmacol. 2024;141:112909.

18. Merker JD, Oxnard GR, Compton C, Diehn M, Hurley P, Lazar AJ, Lindeman N, Lockwood CM, Rai AJ, Schilsky RL. Circulating tumor DNA analysis in patients with cancer: American society of clinical oncology and college of American pathologists joint review. Arch Pathol Lab Med. 2018;142(10):1242–53.
19. Mascarenhas L, Moshel YA, Bayad F, Szentirmai O, Salek AA, Leng LZ, Hofstetter CP, Placantonakis DG, Tsiouris AJ, Anand VK. The transplanum transtuberculum approaches for suprasellar and sellar-suprasellar lesions: avoidance of cerebrospinal fluid leak and lessons learned. World Neurosurg. 2014;82(1–2):186–95.
20. Wen Q, Yang Z, Dai H, Feng A, Li Q. Radiomics study for predicting the expression of PD-L1 and tumor mutation burden in non-small cell lung cancer based on CT images and clinicopathological features. Front Oncol. 2021;11:620246.
21. Song J, Shi J, Dong D, Fang M, Zhong W, Wang K, Wu N, Huang Y, Liu Z, Cheng Y. A new approach to predict progression-free survival in stage IV EGFR-mutant NSCLC patients with EGFR-TKI therapy. Clin Cancer Res. 2018;24(15):3583–92.
22. Deng K, Wang L, Liu Y, Li X, Hou Q, Cao M, Ng NN, Wang H, Chen H, Yeom KW. A deep learning-based system for survival benefit prediction of tyrosine kinase inhibitors and immune checkpoint inhibitors in stage IV non-small cell lung cancer patients: A multicenter, prognostic study. EClinicalMedicine 2022, 51.
23. Mutic S, Dempsey JF. The viewray system: magnetic resonance–guided and controlled radiotherapy. In: Seminars in radiation oncology: 2014: Elsevier; 2014; 196–9.
24. Wang Z-l, Mao L-l, Zhou Z-g, Si L, Zhu H-t, Chen X, Zhou M-j. Sun Y-s, Guo J: Pilot study of CT-Based radiomics model for early evaluation of response to immunotherapy in patients with metastatic melanoma. Front Oncol. 2020;10: 1524.
25. Fan Y, Wang X, Yang C, Chen H, Wang H, Wang X, Hou S, Wang L, Luo Y, Sha X. Brain-Tumor Interface-Based MRI radiomics models to determine EGFR mutation, response to EGFR-TKI and T790M resistance mutation in Non-Small cell lung carcinoma brain metastasis. J Magn Reson Imaging. 2023;58(6):1838–47.
26. Klein S, Staring M, Murphy K, Viergever MA, Pluim JP. Elastix: a toolbox for intensity-based medical image registration. IEEE Trans Med Imaging. 2009;29(1):196–205.
27. Fan L, Yang Z, Chang M, Chen Z, Wen Q. CT-based delta-radiomics nomogram to predict pathological complete response after neoadjuvant chemoradiotherapy in esophageal squamous cell carcinoma patients. J Translational Med. 2024;22(1):579.
28. Lambin P, Rios-Velazquez E, Leijenaar R, Carvalho S, Van Stiphout RG, Granton P, Zegers CM, Gillies R, Boellard R, Dekker A. Radiomics: extracting more information from medical images using advanced feature analysis. Eur J Cancer. 2012;48(4):441–6.
29. He K, Zhang X, Ren S, Sun J. Deep residual learning for image recognition. In: Proceedings of the IEEE conference on computer vision and pattern recognition: 2016;770–778.
30. Feng ZZ, Yang X, Subedi S, McNicholas PD. The LASSO and sparse least squares regression methods for SNP selection in predicting quantitative traits. IEEE/ACM Trans Comput Biol Bioinf. 2011;9(2):629–36.
31. Robin X, Turck N, Hainard A, Tiberti N, Lisacek F, Sanchez J-C, Müller M. pROC: an open-source package for R and S + to analyze and compare ROC curves. BMC Bioinformatics. 2011;12:1–8.
32. Liao C-Y, Lee C-C, Yang H-C, Chen C-J, Chung W-Y, Wu H-M, Guo W-Y, Liu R-S, Lu C-F. Enhancement of radiosurgical treatment outcome prediction using MRI radiomics in patients with non-small cell lung cancer brain metastases. Cancers. 2021;13(16):4030.
33. Chamberlain MC, Baik CS, Gadi VK, Bhatia S, Chow LQ. Systemic therapy of brain metastases: non–small cell lung cancer, breast cancer, and melanoma. Neurooncology. 2017;19(1):i1–24.
34. Han G, Bi J, Tan W, Wei X, Wang X, Ying X, Guo X, Zhou X, Hu D, Zhen W. A retrospective analysis in patients with EGFR-mutant lung adenocarcinoma: is EGFR mutation associated with a higher incidence of brain metastasis? Oncotarget. 2016;7(35):56998.
35. Ge M, Zhuang Y, Zhou X, Huang R, Liang X, Zhan Q. High probability and frequency of EGFR mutations in non-small cell lung cancer with brain metastases. J Neurooncol. 2017;135:413–8.
36. Alvarez-Breckenridge C, Remon J, Piña Y, Nieblas-Bedolla E, Forsyth P, Hendriks L, Brastianos PK. Emerging systemic treatment perspectives on brain metastases: moving toward a better outlook for patients. Am Soc Clin Oncol Educational Book. 2022;42:147–65.
37. Passaro A, Attili I, Morganti S, Del Signore E, Gianoncelli L, Spitaleri G, Stati V, Catania C, Curigliano G, de Marinis F. Clinical features affecting survival in metastatic NSCLC treated with immunotherapy: a critical review of published data. Cancer Treat Rev. 2020;89:102085.
38. Upton DH, Ung C, George SM, Tsoli M, Kavallaris M, Ziegler DS. Challenges and opportunities to penetrate the blood-brain barrier for brain cancer therapy. Theranostics. 2022;12(10):4734.
39. Griffith JI, Rathi S, Zhang W, Zhang W, Drewes LR, Sarkaria JN, Elmquist WF. Addressing BBB heterogeneity: A new paradigm for drug delivery to brain tumors. Pharmaceutics. 2020;12(12):1205.
40. Bai Y, Liu X, Zheng L, Wang S, Zhang J, Xiong S, Zhang P, Jiao Z, Zhao G, Zhou C. Comprehensive profiling of EGFR mutation subtypes reveals genomic-clinical associations in non-small-cell lung cancer patients on first-generation EGFR inhibitors. Neoplasia. 2023;38:100888.
41. Cheng Z, Cui H, Wang Y, Yang J, Lin C, Shi X, Zou Y, Chen J, Jia X, Su L. The advance of the third–generation EGFR–TKI in the treatment of non–small cell lung cancer. Oncol Rep. 2023;51(1):16.
42. Ekman S, Cselényi Z, Varrone A, Jucaite A, Martin H, Schou M, Johnström P, Laus G, Lewensohn R, Brown AP. Brain exposure of osimertinib in patients with epidermal growth factor receptor mutation non-small cell lung cancer and brain metastases: A positron emission tomography and magnetic resonance imaging study. Clin Transl Sci. 2023;16(6):955–65.
43. Malapelle U, Mayo de-Las-Casas C, Rocco D, Garzon M, Pisapia P, Jordana-Ariza N, Russo M, Sgariglia R, De Luca C, Pepe F. Development of a gene panel for next-generation sequencing of clinically relevant mutations in cell-free DNA from cancer patients. Br J Cancer. 2017;116(6):802–10.
44. Garcia-Pardo M, Makarem M, Li JJ, Kelly D, Leighl NB. Integrating circulating-free DNA (cfDNA) analysis into clinical practice: opportunities and challenges. Br J Cancer. 2022;127(4):592–602.
45. Gilson P, Merlin J-L, Harlé A. Deciphering tumour heterogeneity: from tissue to liquid biopsy. Cancers. 2022;14(6):1384.
46. Wang G, Wang B, Wang Z, Li W, Xiu J, Liu Z, Han M. Radiomics signature of brain metastasis: prediction of EGFR mutation status. Eur Radiol. 2021;31:4538–47.
47. Liu Y, Kim J, Qu F, Liu S, Wang H, Balagurunathan Y, Ye Z, Gillies RJ. CT features associated with epidermal growth factor receptor mutation status in patients with lung adenocarcinoma. Radiology. 2016;280(1):271–80.
48. Zhao W, Yang J, Ni B, Bi D, Sun Y, Xu M, Zhu X, Li C, Jin L, Gao P. Toward automatic prediction of EGFR mutation status in pulmonary adenocarcinoma with 3D deep learning. Cancer Med. 2019;8(7):3532–43.
49. Vinod SK, Jameson MG, Min M, Holloway LC. Uncertainties in volume delineation in radiation oncology: a systematic review and recommendations for future studies. Radiother Oncol. 2016;121(2):169–79.
50. Breunig J, Hernandez S, Lin J, Alsager S, Dumstorf C, Price J, Steber J, Garza R, Nagda S, Melian E. A system for continual quality improvement of normal tissue delineation for radiation therapy treatment planning. Int J Radiation Oncology* Biology* Phys. 2012;83(5):e703–8.
51. Nelms BE, Tomé WA, Robinson G, Wheeler J. Variations in the contouring of organs at risk: test case from a patient with oropharyngeal cancer. Int J Radiation Oncology* Biology* Phys. 2012;82(1):368–78.
52. Liu L, Kuang L, Ji Y. Multimodal MRI brain tumor image segmentation using sparse subspace clustering algorithm. Comput Math Methods Med. 2020;2020(1):8620403.
53. Li Y, Lv X, Chen C, Yu R, Wang B, Wang D, Hou D. A deep learning model integrating multisequence MRI to predict EGFR mutation subtype in brain metastases from non-small cell lung cancer. Eur Radiol Experimental. 2024;8(1):2.
54. Ali M, Hu H, Wu T, Mansoor M, Luo Q, Zheng W, Jin N. Segmentation of MRI tumors and pelvic anatomy via cGAN-synthesized data and attention-enhanced U-Net. Pattern Recognit Lett. 2025;187:100–6.
55. Nomura Y, Hanaoka S, Takenaga T, Nakao T, Shibata H, Miki S, Yoshikawa T, Watadani T, Hayashi N, Abe O. Preliminary study of generalized semiautomatic segmentation for 3D voxel labeling of lesions based on deep learning. Int J Comput Assist Radiol Surg. 2021;16:1901–13.
56. Song J, Ding C, Huang Q, Luo T, Xu X, Chen Z, Li S. Deep learning predicts epidermal growth factor receptor mutation subtypes in lung adenocarcinoma. Med Phys. 2021;48(12):7891–9.
57. Nguyen HS, Ho DKN, Nguyen NN, Tran HM, Tam K-W, Le NQK. Predicting EGFR mutation status in non–small cell lung cancer using artificial intelligence: a systematic review and meta-analysis. Acad Radiol. 2024;31(2):660–83.
58. Ahn SJ, Kwon H, Yang J-J, Park M, Cha YJ, Suh SH, Lee J-M. Contrast-enhanced T1-weighted image radiomics of brain metastases May predict EGFR mutation status in primary lung cancer. Sci Rep. 2020;10(1):8905.

59. Zhou Z, Wang M, Zhao R, Shao Y, Xing L, Qiu Q, Yin Y. A multi-task deep learning model for EGFR genotyping prediction and GTV segmentation of brain metastasis. J Translational Med. 2023;21(1):788.
60. Fan Y, Zhao Z, Wang X, Ai H, Yang C, Luo Y, Jiang X. Radiomics for prediction of response to EGFR-TKI based on metastasis/brain parenchyma (M/BP)-interface. Radiol Med. 2022;127(12):1342–54.

Publisher's note

Springer Nature remains neutral with regard to jurisdictional claims in published maps and institutional affiliations.